Journal of Materials Chemistry A

COMMUNICATION

View Article Online
View Journal | View Issue

Cite this: J. Mater. Chem. A, 2017, 5, 6042

Received 20th December 2016
Accepted 20th February 2017

DOI: 10.1039/c6ta10928d

rsc.li/materials-a

Reversible hydrogen storage in yttrium aluminum hydride†

Zhijie Cao,[abc] Liuzhang Ouyang,*[abd] Hui Wang,[ab] Jiangwen Liu,[ab] Michael Felderhoff*[c] and Min Zhu[ab]

Reversible hydrogen storage has been found in transition metal alanates, $Y(AlH_4)_3$, for the first time. An amount of 3.4 wt% H_2 can be released at 140 °C from the first dehydrogenation step of $Y(AlH_4)_3$, and 75% of it is reversible at 145 °C and 100 bar H_2, which holds promise for low-temperature applications.

Pure hydrogen is an ideal energy source for proton exchange membrane (PEM) fuel cell vehicles. However, large-scale hydrogen application in the field of PEM fuel cells, especially for those with operating temperatures below 100 °C, is limited due to the absence of a safe and effective hydrogen storage approach.[1,2] A possible solution could be a novel hybrid tank system, which combines a high-pressure tank with unstable metal hydrides. This system shows obvious advantages in terms of gravimetric and/or volumetric hydrogen density compared to high pressure, solid state or liquid hydrogen storage techniques.[3]

Unstable metal hydrides for hybrid tank systems have the characteristic of high desorption plateau pressures, meaning that they don't exist under ambient conditions (room temperature, 1 bar pressure). This high desorption plateau pressure is the result of a decomposition enthalpy (ΔH) of the metal hydrides of less than 20 kJ mol^{-1} H_2. Consequently, these unstable hydrides can be synthesized only at low temperatures and/or under very high hydrogen pressure conditions.[4] To achieve needs for future metal hydride/fuel cell applications, it is important to consider the overall system performance and not just the properties of materials. Nevertheless, large hydrogen capacity, sufficient kinetics at low temperatures and excellent long-term stability are also very important material properties. To date, several unstable metal hydrides including AB_2-type[5–7] and V-based BCC alloys[8,9] have been investigated for a hybrid tank system. Until now, their reversible hydrogen capacity (<2 wt%) is too low to meet practical requirements. It is believed that an unstable metal hydride with a reversible capacity of 4 wt% can bring this hybrid system close to an attractive level.[10] However, novel unstable hydrides like light weight alloys or complex hydride systems with higher hydrogen capacity are more favorable.

During the past two decades, light complex aluminium hydrides like $NaAlH_4$, $LiAlH_4$, $KAlH_4$, *etc.*, have been intensively investigated as potential candidates for solid-state hydrogen storage due to their relatively high capacity, moderate absorption/desorption conditions and good reversibility in the presence of catalysts.[11–15] For example, $TiCl_3$-doped $NaAlH_4$ showed a high reversible capacity of ~4 wt% H_2 during 100 de/rehydrogenation cycles at relatively low temperatures of 70 and 270 °C.[11] On the other hand, $LiAlH_4$ can't be synthesized directly in the solid state from commercially available LiH and Al powders. The synthesis is only possible in an ether solution. $LiAlH_4$ can release more than 7 wt% H_2 with an onset dehydrogenation temperature of 80 °C, and the dehydrogenated sample can be recycled in an ether solution with a retention capacity of 6.4 wt% even after 3 cycles.[12] For these light aluminium hydrides, the hydrogen capacities of the first decomposition steps are not sufficient, while the decomposition temperatures for the second decomposition steps are too high, which makes them inappropriate for low temperature fuel cells.[16] Besides these light aluminium hydrides, several thermodynamically unstable transition metal aluminium hydrides with a high hydrogen content like $Ti(AlH_4)_4$ (9.3 wt% H_2), $Fe(AlH_4)_2$ (5.8 wt% H_2), or $Y(AlH_4)_3$ (6.6 wt% H_2) are described, but have attracted less attention.[17] The general synthesis of these transition metal complex aluminium hydrides $M(AlH_4)_n$ (M = Ti, V, Co, Mn, Fe, Cu, Zr, Nb, Ag, Ce, Ta, *etc.*) was carried out at very low temperatures

[a]School of Materials Science and Engineering, Key Laboratory of Advanced Energy Storage Materials of Guangdong Province, South China University of Technology, Guangzhou, 510641, PR China. E-mail: meouyang@scut.edu.cn; Fax: +86-20-87112762

[b]China-Australia Joint Laboratory for Energy & Environmental Materials, South China University of Technology, Guangzhou, 510641, PR China

[c]Max-Planck-Institut für Kohlenforschung, Kaiser-Wilhelm-Platz 1, 45470 Mülheim an der Ruhr, Germany. E-mail: felderhoff@mpi-muelheim.mpg.de; Tel: +49-2083062368

[d]Key Laboratory for Fuel Cell Technology in Guangdong Province, Guangzhou, 510641, PR China

† Electronic supplementary information (ESI) available. See DOI: 10.1039/c6ta10928d

between −110 and −80 °C because the decomposition and hydrogen release start in most cases at −50 °C or below.[18] For instance, $Ti(AlH_4)_4$ and $Fe(AlH_4)_2$ start to decompose slowly above −80 °C and two hydrogen atoms are liberated while heating to room temperature.[19] Compounds $[RE(AlH_4)_3]$ (RE = La, Ce, Pr) already start to evolve hydrogen and form RE aluminium hydride $REAlH_6$ and Al metal during the ball milling process of rare earth chlorides and sodium aluminium hydride.[16] Among all these transition metal complex aluminium hydrides, the relatively high stability of $TaH_2(AlH_4)_2$ and $Y(AlH_4)_3$ is remarkable.[20–22] The thermal decomposition of $TaH_2(AlH_4)_2$ occurs in the interval of 135–195 °C, and the metal–hydrogen bonds are even retained after hydrolysis.[20,21] $Y(AlH_4)_3$ was reported to be quite stable and starts to decompose at 50 °C.[22] $Y(AlH_4)_3$ has a high theoretical hydrogen content of 6.6 wt%, while until now no further information is known about its hydrogen storage properties and reversibility. In this work, in order to continue to explore new unstable high capacity hydrides (>4 wt%), $Y(AlH_4)_3$ was prepared *via* a mechanochemical reaction. The dehydrogenation mechanism, hydrogen storage properties, reversibility and prospect for hydrogen storage were systematically evaluated. The preliminary results of the kinetics and reversibility of this alanate are quite interesting, which encourages us to place more effort into exploring new types of unstable hydrides with favorable hydrogen storage properties.

The mechanochemical metathesis reaction is a convenient and efficient procedure for the synthesis of complex aluminium hydrides.[23] Fig. 1(a) presents the XRD patterns of the as-milled YCl_3–$3LiAlH_4$ mixture and $LiAlH_4$ milled under the same conditions. For comparison the XRD pattern of the blank sample stage was also presented. Pure $LiAlH_4$ remains in a highly crystalline state after ball milling for 6 h. For the as-milled YCl_3–$3LiAlH_4$ mixture, an exchange reaction between $3LiAlH_4$ and YCl_3 initiated by ball milling would theoretically lead to the formation of $Y(AlH_4)_3$ and 3LiCl, while here only the diffraction peaks of LiCl can be observed with the absence of any other phases. Moreover, it is noteworthy that the background intensity of the as-milled YCl_3–$3LiAlH_4$ sample between 26° and 36° is obviously higher than that of the blank sample stage, suggesting a possible amorphous nature of $Y(AlH_4)_3$. Actually the amorphous structure was verified after the removal of LiCl *via* an extraction with diethylether and drying procedure (Fig. S1†). This result is consistent with the observation by Kost *et al.*,[22] who also demonstrated the amorphous nature of $Y(AlH_4)_3$. As shown in Fig. S1,† the presence of traceable diffraction peaks of Al indicated a minimal decomposition of $Y(AlH_4)_3$ during the purification process. Most of the transition tetrahydroaluminates $M(AlH_4)_n$ decompose at −50 °C or even below while yttrium tetrahydroaluminate is an exception.[18] The appearance of the diffraction peaks of Al metal and the increase of pressure inside the jar during the milling process implied the decomposition of unstable $RE(AlH_4)_3$ hydrides.[16] In this study, $Y(AlH_4)_3$ still stays in an amorphous state after ball milling without the observation of any decomposition products, further confirming its relatively high stability under normal conditions. Fig. 1(b) shows the FT-IR patterns of the as-milled $LiAlH_4$ and YCl_3–$3LiAlH_4$ sample. The as-milled $LiAlH_4$ shows two Al–H stretching vibration frequencies at 1785 cm^{-1} and 1645 cm^{-1}, consistent with the reported values (1757 cm^{-1} and 1615 cm^{-1}).[24] In the fingerprint region, the bands at 885, 790, and 704 cm^{-1} correspond to the deformational modes; meanwhile the combination band is at 1450 cm^{-1}.[25] The shift of the Al–H stretching band towards a higher frequency (about 30 cm^{-1}) in the spectrum of the as-milled $LiAlH_4$ was thought to be related to the strain effect induced by milling treatment,[26] which was also observed in the as-milled $KAlH_4$ (ref. 27) and $LiAlH_4$ under a high static pressure (GPa).[28] Distinct differences exist in the FT-IR spectra of the as-milled YCl_3–$3LiAlH_4$ and $LiAlH_4$ due to the different chemical environments of the Al–H bonds. The as-milled YCl_3–$3LiAlH_4$ sample exhibits only one stretching vibration (1800 cm^{-1}) and one broad deformational band at 690 cm^{-1} for the Al–H bond. The peak at 1640 cm^{-1} corresponds to the water bending vibration.[29] No bands for the $LiAlH_4$ can be detected in the FT-IR spectrum of the YCl_3–$3LiAlH_4$ sample, implying the complete transformation from the starting materials into the product (a mixture of $Y(AlH_4)_3$ and 3LiCl, donates as $Y(AlH_4)_3$–3LiCl) after 6 h of ball milling. Such a result is in good agreement with the results of XRD analysis.

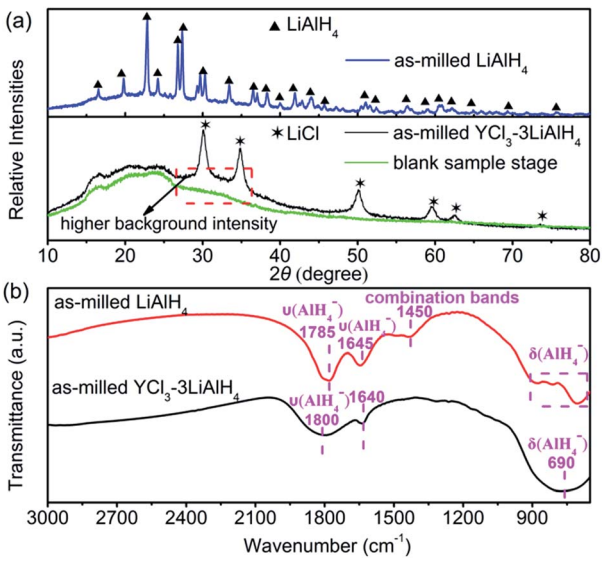

Fig. 1 (a) XRD patterns and (b) FT-IR spectra of the as-milled $LiAlH_4$ and YCl_3–$3LiAlH_4$ sample.

The thermal dehydrogenation properties of $Y(AlH_4)_3$ were measured by TPD, MS and DSC, and the results are shown in Fig. 2. Three endothermic dehydrogenation peaks are observed during the heating process. All these dehydrogenation peaks combined with the release of hydrogen gas. These three steps with different slopes can be distinguished in the TPD volumetric release curve (labeled with a serial number). One additional exothermic peak at ~395 °C can be observed in the DSC curve, besides the aforementioned three endothermic dehydrogenation stages (as shown by arrows). These results indicate that altogether four different steps are involved in the thermal decomposition process of $Y(AlH_4)_3$. As shown in the TPD curve, hydrogen release from $Y(AlH_4)_3$ starts at around 80 °C, accelerates at ~120 °C and first peaks at ~140 °C. The first

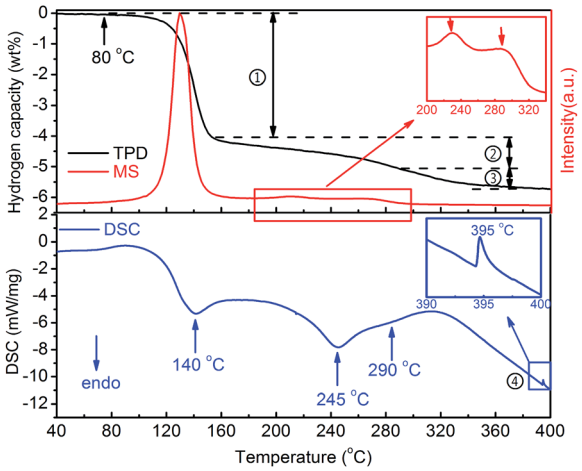

Fig. 2 TPD, MS and DSC curves of the $Y(AlH_4)_3$–3LiCl sample. The wt% H_2 values are normalized to the $Y(AlH_4)_3$ percentage.

dehydrogenation stage is finished at ~170 °C with a desorption capacity of ~3.9 wt% H_2. In the temperature range from 170 to 350 °C, two dehydrogenation reactions with maxima at 245 °C and 290 °C can be observed. The quantitative measurement of these two processes delivers a hydrogen amount of ~1.0 wt% and ~0.7 wt%, respectively. A total hydrogen amount of ~5.6 wt% H_2 can be released from the $Y(AlH_4)_3$ within the temperature range of 80–400 °C. These desorbed hydrogen values were normalized to reflect the weight of $Y(AlH_4)_3$ (overall hydrogen amount is 6.6 wt%) considering the theoretical ratio of $Y(AlH_4)_3$ and LiCl (1 : 3) in the ball milled product.

For further understanding thermal decomposition of $Y(AlH_4)_3$, XRD analyses of the dehydrogenated samples at different temperatures were performed (see Fig. 3). Kost *et al.* proposed that, thermal decomposition of $Y(AlH_4)_3$ proceeds directly through YH_3 and AlH_3 derived on the basis of evolved hydrogen capacity and thermographic data.[22] However, here only the characteristic diffraction pattern of Al metal arises after

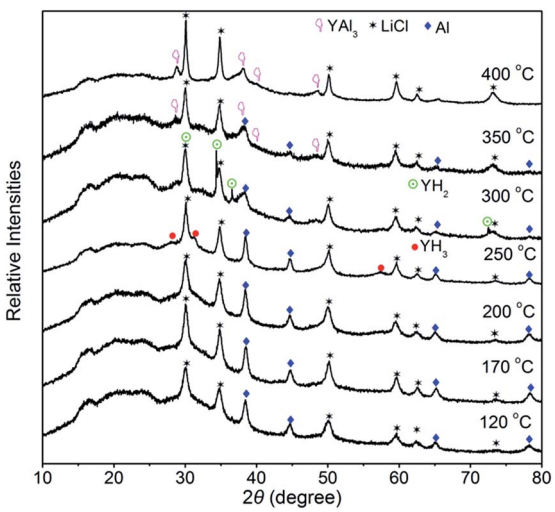

Fig. 3 XRD patterns of the dehydrogenated samples at different stages.

dehydrogenation at 120 °C, and no information concerning these reported intermediates can be detected. This result suggests that the dehydrogenation $Y(AlH_4)_3$ maybe occur in a way different from this description. The generally accepted decomposition pathway of aluminium tetrahydrides is a two-stage reaction. Starting from AlH_4^- units an aluminium hexahydride compound in combination with aluminium metal is produced in the first step. Afterwards the hexahydride compound decomposes into a metal hydride and aluminium metal. For metal elements in their stable +1 and +3 oxidation states, the intermediates would be M_3AlH_6 (M = Li, Na, K)[15] or $MAlH_6$ (M = RE),[16] while for the stable +2 oxidation state, these hydrides usually formed compounds with the formula $MAlH_5$.[23,30] For instance, a new intermediate $MeAlH_5$ (Me = Eu, Sr) with a zigzag chain formed by corner-sharing octahedra was identified during the decomposition process of the complex aluminium hydride, $Me(AlH_4)_2$.[31] For unstable $RE(AlH_4)_3$ hydrides, a $REAlH_6$ intermediate compound with isolated octahedra altering with the RE cations is formed before transforming to REH_x hydrides.[16] Here in $Y(AlH_4)_3$, however, no other Y–Al–H containing decomposition products can be identified even up to the temperature range between 170 °C and 200 °C by means of XRD, suggesting that this new $YAlH_x$ hydride may also be amorphous. We propose this $YAlH_x$ hydride to be $YAlH_6$ based on two reasons: (1) the yttrium element has a stable +3 oxidation state, which is more likely to result in the formation of $[AlH_6]^{3-}$; (2) for the formation of the hexahydride, 50% of the hydrogen was expected to be released from the first dehydrogenation step.[16] According to the TPD curve of $Y(AlH_4)_3$ in Fig. 2, a capacity of ~3.9 wt% H_2 (59% of the total hydrogen) is liberated from the first desorption reaction, which is in reasonable agreement with the results observed for the first dehydrogenation step of $RE(AlH_4)_3$ (La 51%, Ce 60%, Pr 56%, and Nd 57%) with $REAlH_6$ as the intermediate phase.[16] With further increase of the temperature to 250 °C, diffraction peaks of YH_3 show up; meanwhile the intensities of visible free Al metal obviously increase. This result demonstrates that the newly formed $YAlH_6$ decomposes into YH_3, Al and H_2 during the second dehydrogenation stage. Above 250 °C, YH_3 starts to transform into YH_2 and H_2. When the temperature increases to 300 °C, the diffraction peaks of YH_3 disappear and only those of YH_2 can be observed. As the temperature reaches 350 °C, it is noted that the diffraction peaks of YH_2 completely disappear and the intensity of free Al metal also significantly decreases. Meanwhile new intermetallic YAl_3 is formed, which results from the reaction between YH_2 and Al. Further heating the sample up to 400 °C results in the complete dehydrogenation of YH_2; hence YAl_3 is dominant in the XRD pattern.

According to the above analysis, $Y(AlH_4)_3$ is most probably made up of isolated tetrahedral $[AlH_4]^-$, while the intermediate decomposition product consists of octahedral $[AlH_6]^{3-}$, which is very similar to the crystal structure of $REAlH_6$.[16] Therefore, the experimental results obtained in the present case suggest a reaction mechanism as follows:

$$\text{First step (80–170 °C): } Y(AlH_4)_3 \rightarrow YAlH_6 + 2Al + 3H_2$$

Second step (170–250 °C): $YAlH_6 \rightarrow YH_3 + Al + 1.5H_2$

Third step (250–350 °C): $YH_3 \rightarrow YH_2 + 0.5H_2$

Fourth step (>350 °C): $YH_2 + 3Al \rightarrow YAl_3 + H_2$

It must be mentioned that other intermediates of the general formula YAl_xH_y can't be excluded, which leads to the fact that the overall hydrogen capacity is reduced and that these intermediates may contribute to additional dehydrogenation steps.

To realize the low temperature (25–150 °C) application of $Y(AlH_4)_3$ in hybrid tanks, only the first dehydrogenation step can be possible. Thus isothermal desorption kinetic curves of $Y(AlH_4)_3$ in a temperature range from 80 to 140 °C were studied, and the results are displayed in Fig. S3.† The wt% H_2 values are normalized to the $Y(AlH_4)_3$ percentage. $Y(AlH_4)_3$ can release ~3.4 wt% H_2 within 60 min at 140 °C, and ninety percent of the hydrogen can be liberated in 30 min at this temperature. The activation energy for the dehydrogenation process of $Y(AlH_4)_3$ is estimated to be 91.7 kJ mol^{-1} (Fig. S3d†), which is much smaller compared to that of other nanocrystalline complex metal alanates, *e.g.* rod $Mg(AlH_4)_2$ with 123.0 kJ mol^{-1}.[32] A possible explanation for the low on-set dehydrogenation temperature of 80 °C could be this low kinetic barrier.

After dehydrogenation at 145 °C, a series of recharge/discharge experiments were performed to demonstrate the reversibility of the first dehydrogenation step of $Y(AlH_4)_3$. After each dehydrogenation, the samples were rehydrogenated at a pressure of 100 bar H_2, and afterwards dehydrogenated in a vacuum at the same temperature. Fig. 4 shows the isothermal (a) absorption and (b) desorption kinetic curves of $Y(AlH_4)_3$ for three consecutive cycles at 145 °C. As shown in Fig. 4(a), during rehydrogenation cycles an amount of ~2.6 wt% H_2 can be absorbed at 145 °C and the whole amount of absorbed hydrogen can be liberated during the corresponding dehydrogenation processes (Fig. 4(b)). In general, the reversible hydrogen storage capacity at 145 °C can reach 2.6 wt%, indicating the reversibility of the first dehydrogenation step of $Y(AlH_4)_3$. This corresponds to ~75% of the theoretical hydrogen capacity of $Y(AlH_4)_3$ for the first step. To our knowledge, this is the first time that reversible hydrogen storage is found in any transition metal alanates. To check whether $Y(AlH_4)_3$ has a higher reversibility or not, its final thermal decomposition product (YAl_3) was prepared, and was subjected to a high pressure of 300 bar. As shown in Fig. S5,† not any exothermic peaks for hydrogen absorption can be observed, indicating that the YAl_3 alloy can't absorb hydrogen in a temperature range from −40 °C to 100 °C and at a high pressure of 300 bar. This is also the case for the YH_3 + 3Al mixture, which cannot be hydrogenated at a pressure of 100 bar H_2 at 145 °C (Fig. S6†). These results demonstrate that only the first dehydrogenation step of $Y(AlH_4)_3$ can be rehydrogenated. Further attempts to improve the reversibility of unstable transition complex alanates are underway in our laboratories.

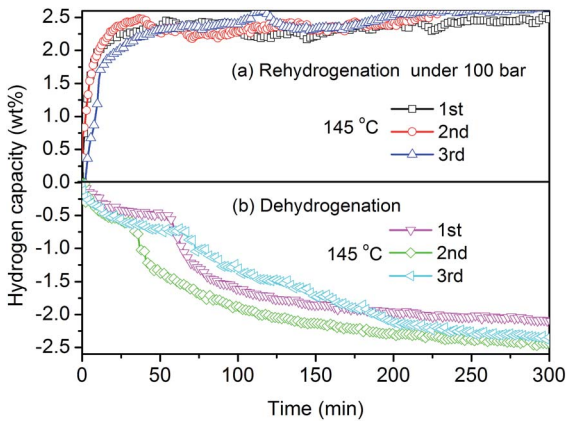

Fig. 4 (a) Isothermal absorption and (b) desorption kinetic curves of $Y(AlH_4)_3$ for three consecutive cycles at 145 °C. The wt% H_2 values are normalized to the $Y(AlH_4)_3$ percentage.

Conclusions

A new complex metal aluminium hydride with the composition of $Y(AlH_4)_3$ was prepared *via* the mechanochemical reaction of $YCl_3 + 3LiAlH_4$. Upon heating, the $Y(AlH_4)_3$ sample decomposes *via* a four-stage dehydrogenation process over the temperature range of 80–400 °C. At 80–170 °C, $Y(AlH_4)_3$ is first decomposed into an intermediate hydride, $YAlH_6$, 2Al and $3H_2$. With increasing temperature up to 250 °C, $YAlH_6$ continues to release hydrogen to form YH_3 and additional Al metal. Upon further increasing the temperature to 300 °C, YH_3 starts to decompose into YH_2 and H_2. As the temperature reaches 350 °C, the newly formed YH_2 starts to react with Al to generate YAl_3, and this reaction proceeds completely upon further heating the sample up to 400 °C. An amount of 3.4 wt% H_2 can be released from the sample within ~60 min at 140 °C during the first dehydrogenation step. The apparent activation energy of the first dehydrogenation step of $Y(AlH_4)_3$ is 92.1 kJ mol^{-1}. Rehydrogenation experiments indicate that the first dehydrogenation step shows a reversibility of 75% even at a low temperature of 145 °C. This is the first example that a transition metal alanate can reversibly absorb hydrogen. Further improvements on the hydrogen storage properties of $Y(AlH_4)_3$ would make it a possible and promising candidate for hybrid tank system applications.

Acknowledgements

This work was supported by the Foundation for Innovative Research Groups of the National Natural Science Foundation of China (No. NSFC51621001), National Natural Science Foundation of China Projects (No. 51431001), by the International Science & Technology Cooperation Program of China (2015DFA51750) and by the Project Supported by the Natural Science Foundation of Guangdong Province of China (2014GKXM011 and 2014A030311004). The Project Supported by Guangdong Province Universities and Colleges Pearl River Scholar Funded Scheme (2014) is also acknowledged. The support from the China Scholarship Council is specially acknowledged. Open Access funding provided by the Max Planck Society.

Notes and references

1 P. M. Grant, *Nature*, 2003, **424**, 129–130.
2 L. Schlapbach and A. Züttel, *Nature*, 2001, **414**, 353–358.
3 N. Takeichi, H. Senoh, T. Yokota, H. Tsuruta, K. Hamada, H. T. Takeshita, H. Tanaka, T. Kiyobayashi, T. Takano and N. Kuriyama, *Int. J. Hydrogen Energy*, 2003, **28**, 1121–1129.
4 C. Weidenthaler and M. Felderhoff, *Energy Environ. Sci.*, 2011, **4**, 2495–2502.
5 Z. Chen, X. Xiao, L. Chen, X. Fan, L. Liu, S. Li, H. Ge and Q. Wang, *J. Alloys Compd.*, 2014, **585**, 307–311.
6 Z. Cao, L. Ouyang, H. Wang, J. Liu, D. Sun, Q. Zhang and M. Zhu, *Int. J. Hydrogen Energy*, 2015, **40**, 2717–2728.
7 Z. Cao, L. Ouyang, H. Wang, J. Liu, L. Sun and M. Zhu, *J. Alloys Compd.*, 2015, **639**, 452–457.
8 T. Matsunaga, M. Kon, K. Washio, T. Shinozawa and M. Ishikiriyama, *Int. J. Hydrogen Energy*, 2009, **34**, 1458–1462.
9 T. Kuriiwa, T. Maruyama, A. Kamegawa and M. Okada, *Int. J. Hydrogen Energy*, 2010, **35**, 9082–9087.
10 D. Mori and K. Hirose, *Int. J. Hydrogen Energy*, 2009, **34**, 4569–4574.
11 B. Bogdanović and M. Schwickardi, *J. Alloys Compd.*, 1997, **253–254**, 1–9.
12 X. Liu, H. W. Langmi, S. D. Beattie, F. F. Azenwi, G. S. McGrady and C. M. Jensen, *J. Am. Chem. Soc.*, 2011, **133**, 15593–15597.
13 R. Gremaud, A. Borgschulte, W. Lohstroh, H. Schreuders, A. Züttel, B. Dam and R. Griessen, *J. Alloys Compd.*, 2005, **404–406**, 775–778.
14 B. Bogdanović, M. Felderhoff, A. Pommerin, F. Schüth and N. Spielkamp, *Adv. Mater.*, 2006, **18**, 1198.
15 S. I. Orimo, Y. Nakamori, J. R. Eliseo, A. Züttel and C. M. Jensen, *Chem. Rev.*, 2007, **107**, 4111–4132.
16 C. Weidenthaler, A. Pommerin, M. Felderhoff, W. Sun, C. Wolverton, B. Bogdanović and F. Schüth, *J. Am. Chem. Soc.*, 2009, **131**, 16735–16743.
17 H. Neumaier, D. Büchel and G. Ziegelmaier, *Z. Anorg. Allg. Chem.*, 1966, **345**, 46–52.
18 G. L. Soloveichik and B. M. Bulychev, *Russ. Chem. Rev.*, 1983, **52**, 43–60.
19 M. E. Kost and A. L. Golovanova, *Russ. Chem. Bull.*, 1975, **24**, 905–907.
20 A. I. Golovanova, M. E. Kost and V. I. Mikheeva, *Russ. Chem. Bull.*, 1973, **22**, 1410–1413.
21 A. I. Golovanova, M. E. Kost and V. I. Mikheeva, *Izv. Akad. Nauk SSSR*, 1973, **5**, 1448–1452.
22 M. E. Kost and A. I. Golvanova, *Inorg. Mater.*, 1978, **14**, 1348–1350.
23 M. Mamatha, B. Bogdanović, M. Felderhoff, A. Pommerin, W. Schmidt, F. Schüth and C. Weidenthaler, *J. Alloys Compd.*, 2006, **407**, 78–86.
24 C. Li, X. Xiao, L. Chen, K. Jiang, S. Li and Q. Wang, *J. Alloys Compd.*, 2011, **509**, 590–595.
25 J. R. Ares, K. F. Aguey-Zinsou, F. Leardini, I. J. Ferrer, J. F. Fernandez, Z. X. Guo and C. Sánchez, *J. Phys. Chem. C*, 2009, **113**, 6845–6851.
26 J. R. Ares, K. F. Aguey-Zinsou, M. Porcu, J. M. Sykes, M. Dornheim, T. Klassen and R. Bormann, *Mater. Res. Bull.*, 2008, **43**, 1263–1275.
27 J. R. Ares Fernandez, F. Aguey-Zinsou, M. Elsaesser, X. Z. Ma, M. Dornheim, T. Klassen and R. Bormann, *Int. J. Hydrogen Energy*, 2007, **32**, 1033–1040.
28 A. V. Talyzin and B. Sundqvist, *Phys. Rev. B: Condens. Matter Mater. Phys.*, 2004, **70**, 180101.
29 X. Z. Xiao, C. X. Li, L. X. Chen, X. L. Fan, H. Q. Kou and Q. D. Wang, *J. Alloys Compd.*, 2011, **509**, S743–S746.
30 A. Marashdeh and T. J. Frankcombe, *J. Chem. Phys.*, 2008, **128**, 234505.
31 A. Pommerin, A. Wosylus, M. Felderhoff, F. Schüth and C. Weidenthaler, *Inorg. Chem.*, 2012, **51**, 4143–4150.
32 Y. Liu, Y. Pang, X. Zhang, Y. Zhou, M. Gao and H. Pan, *Int. J. Hydrogen Energy*, 2012, **37**, 18148–18154.

